



Oxocarbon Salts for Fast Rechargeable Batteries

Qing Zhao, Jianbin Wang, Yong Lu, Yixin Li, Guangxin Liang, and Jun Chen*

Abstract: Oxocarbon salts ($M_2(\text{CO})_n$) prepared through one-pot proton exchange reactions with different metal ions ($M = \text{Li, Na, K}$) and frameworks ($n = 4, 5, 6$) have been rationally designed and used as electrodes in rechargeable Li, Na, and K-ion batteries. The results show that $M_2(\text{CO})_5/M_2(\text{CO})_6$ salts can insert two or four metal ions reversibly, while $M_2(\text{CO})_4$ shows less electrochemical activity. Especially, we discover that the $\text{K}_2\text{C}_6\text{O}_6$ electrode enables ultrafast potassium-ion insertion/extraction with 212 mA h g^{-1} at 0.2 C and 164 mA h g^{-1} at 10 C . This behavior can be ascribed to the natural semiconductor property of $\text{K}_2\text{C}_6\text{O}_6$ with a narrow band gap close to 0.9 eV , the high ionic conductivity of the K-ion electrolyte, and the facilitated K-ion diffusion process. Moreover, a first example of a K-ion battery with a rocking-chair reaction mechanism of $\text{K}_2\text{C}_6\text{O}_6$ as cathode and $\text{K}_4\text{C}_6\text{O}_6$ as anode is introduced, displaying an operation voltage of 1.1 V and an energy density of 35 Wh kg^{-1} . This work provides an interesting strategy for constructing rapid K-ion batteries with renewable and abundant potassium materials.

Building better battery systems with advanced and renewable materials is essentially significant for future energy storage and conversion of human society.^[1] Among the considerable efforts on developing novel electrode materials with earth-abundant elements, organic electrode materials have revealed powerful competence owing to their intrinsic designability, high abundance, and sustainability.^[2] A target issue that needs to be resolved for organic electrode materials such as quinones is their high solubility in aprotic electrolyte, which results in fast capacity/cycling decay of rechargeable batteries.^[3] Throughout the various strategies on conquering this problem, the design of “inorganic/organic” hybrid materials (metalorganic salts) is intriguing.^[4] This type of hybrid materials endowed with high polarity and intermolecular chelate bonds exhibits less solubility in aprotic electrolyte, maintaining an ameliorative cycling life. Up to now, a series of organic salts with functional groups of metal enolate ($-\text{OLi}$, $-\text{ONa}$),^[5] metal carboxylate ($-\text{COOLi}$, $-\text{COONa}$)^[6] and sulfonate ($-\text{SO}_3\text{Na}$)^[7] have been applied for rechargeable lithium and sodium batteries.

Oxocarbon, which has been first introduced in 1963, can be regarded as the polycarbonyl compounds.^[8] The carbonyl is redox center of cation (H^+ , Li^+ , Na^+ , K^+ , Mg^{2+}) insertion/extraction.^[2c] Thus, the oxocarbon compounds with salted substituents will process the superiorities of high theoretic capacity and low dissolution. In 2008, $\text{Li}_2\text{C}_6\text{O}_6$ was initially investigated as a high capacity cathode for rechargeable lithium batteries, displaying a high capacity of 580 mA h g^{-1} in the first cycle.^[5a] After that, other oxocarbon salts such as $\text{Na}_2\text{C}_5\text{O}_5$ and $\text{Na}_2\text{C}_6\text{O}_6$ were also reported in rechargeable lithium and sodium batteries.^[5d–g] These previous studies have verified the potential interest of oxocarbon salts for energy storage, while the comprehensive investigation of oxocarbon salts with various frameworks/substituents is still limited. Meanwhile, the accommodating ability of big cations such as the K ion with oxocarbon salts is also unexploited.

Benefiting from the widespread K-ion transport, high abundance of K resource, and low standard electric potential of K^+/K , the rechargeable K-based batteries have been paid durable attention, while the study of proper hosts for inserting large K ions ($r(\text{K}^+) = 152 \text{ pm}$, $r(\text{Li}^+) = 73 \text{ pm}$) is still challenging.^[9] The electrochemical redox behavior with organic carbonyl compounds is based on a conversion reaction, which is less limited by the cation radius^[10] and hence provides the possibility of affording the bigger K-ion. Moreover, with an elaborate design of substituents, the oxocarbon salt also offers the opportunity of constructing an all-organic rocking-chair K-ion battery without using the risky metal potassium.

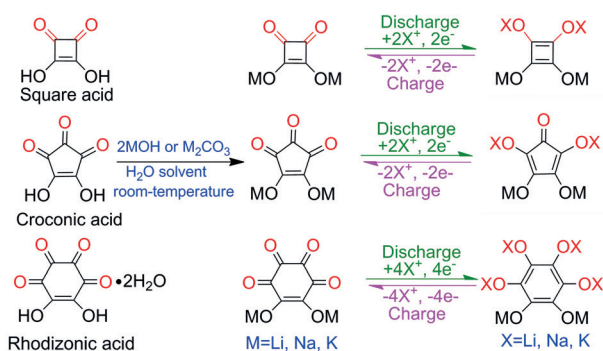
Herein, nine oxocarbon salts of $M_2(\text{CO})_n$ ($M = \text{Li, Na, K}$, $n = 4, 5, 6$) with tailored frameworks and substituents are rationally designed for rechargeable batteries. With different metals as anodes ($\text{Li}_2(\text{CO})_n$ with Li anode; $\text{Na}_2(\text{CO})_n$ with Na anode; $\text{K}_2(\text{CO})_n$ with K anode), the electrochemical properties of these nine salts are systematically investigated and compared. The four-membered ring salts have difficulties to take up metal ions in a selected voltage region. The five/six-membered ring salts are feasible to take up a certain number of metal ions. Remarkably, we firstly found that $\text{K}_2\text{C}_6\text{O}_6$ (or $\text{K}_2\text{C}_5\text{O}_5$) can be applied as an ultrafast K-ion insertion/extraction host with two K-ion reactions per compound. The discharge capacity of $\text{K}_2\text{C}_6\text{O}_6$ is 212 mA h g^{-1} at 0.2 C and 164 mA h g^{-1} at a higher rate of 10 C . DFT calculations show that $\text{K}_2\text{C}_6\text{O}_6$ is a semiconductor with a narrow band gap close to 0.9 eV . Moreover, the K-ion electrolyte processes natural higher ionic conductivity than Li/Na-ion electrolyte. Meanwhile, K-ion in $\text{K}_2\text{C}_6\text{O}_6$ also shows faster diffusion than Li/Na-ion in $\text{Li}_2\text{C}_6\text{O}_6/\text{Na}_2\text{C}_6\text{O}_6$. As a pioneer, the K-ion battery with $\text{K}_2\text{C}_6\text{O}_6$ as cathode and $\text{K}_4\text{C}_6\text{O}_6$ as anode was constructed and exhibited an energy density of 35 Wh kg^{-1} .

The organic oxocarbon salts with active carbonyl compounds (Scheme 1) were obtained in simple one-pot proton

[*] Dr. Q. Zhao, Dr. J. Wang, Dr. Y. Lu, Dr. Y. Li, Prof. G. Liang, Prof. J. Chen
Key Laboratory of Advanced Energy Materials Chemistry and State Key Laboratory of Elemento-Organic Chemistry
College of Chemistry, Nankai University, Tianjin 300071 (China)
E-mail: chenabc@nankai.edu.cn

Prof. J. Chen
Collaborative Innovation Center of Chemical Science and Engineering, Nankai University Tianjin 300071 (China)

Supporting information for this article can be found under: <http://dx.doi.org/10.1002/anie.201607194>.



Scheme 1. Preparation, structures, and theoretic reactions of designed oxocarbon salts.

exchange reactions. In brief, $\text{M}_2\text{C}_4\text{O}_4$, $\text{M}_2\text{C}_5\text{O}_5$, and $\text{M}_2\text{C}_6\text{O}_6$ were prepared by reactions of square acid ($\text{H}_2\text{C}_4\text{O}_4$), croconic acid ($\text{H}_2\text{C}_5\text{O}_5$), and rhodizonic acid ($\text{H}_2\text{C}_6\text{O}_6 \cdot 2\text{H}_2\text{O}$) and the corresponding hydroxide (MOH) or carbonates (M_2CO_3) in water as solvent, respectively (experiment details are given in the Supporting Information). In addition, the excess annealing process is necessary to remove crystal water from some products ($\text{Li}_2\text{C}_5\text{O}_5$ and $\text{Li}_2\text{C}_6\text{O}_6$). The structures, morphologies, thermostabilities of the prepared composites were confirmed and characterized with Fourier Transform infrared spectroscopy (FTIR), X-ray powder diffraction (XRD), scanning electron microscope (SEM), and thermogravimetry analysis (TG) (see Figures S1–S6 in the Supporting Information). All prepared oxocarbon salts exhibit high crystallinity and thermostability (up to 300°C). Typical vibrations belong-

ing to C=C bonds and C=O bonds can be detected in the FTIR spectra. In general, the particle size of the as-prepared compounds ranges from several hundred nanometers to several micrometers. Meanwhile, most oxocarbon salts are hardly soluble in organic electrolyte (Figure S7).

The batteries were tested with different metals, such as Li, Na, and K, as anodes and oxocarbon salts as cathodes. The carbonyl activities with initial discharge capacities are summarized in Figure 1a. The four-membered ring salts show an ignorable capacity after eliminating the contribution of Super P conducting additive (Figure S8a–f). This result suggests that the four-membered ring oxocarbon salts are unable to insert enough metal ions. The steric hindrance or electrostatic repulsion is considered primarily responsible. In comparison, five-membered oxocarbon salts can insert about two metal-ions (Li^+ , Na^+ , and K^+) in the first cycle (Figure S9a–9d). Among them, the Li/ $\text{Li}_2\text{C}_5\text{O}_5$ battery displays the highest operation potential due to the lower standard potential of Li^+/Li and less electron-donating properties of the $-\text{OLi}$ group. The six-membered ring cathode reveals high reversibility. The Li/ $\text{Li}_2\text{C}_6\text{O}_6$ battery is able to take up four Li ions with an initial capacity close to 580 mA h g^{-1} . The capacity fades fast with cycling and only a capacity of less than 300 mA h g^{-1} is obtained after 10 cycles owing to the exfoliation of the C_6O_6 layers (Figure S10a).^[5b] As a comparison, Na/ $\text{Na}_2\text{C}_6\text{O}_6$ (Figure S10b) and K/ $\text{K}_2\text{C}_6\text{O}_6$ (Figure S10c) batteries can take up two electrons and metal ions. In addition, the capacity of $\text{K}_2\text{C}_6\text{O}_6$ decays only by 0.4 % per cycle from the 2nd to 100th cycling (Figure S11). When the operation voltage is widened, the use of carbonyl compounds in $\text{Na}_2\text{C}_6\text{O}_6$ and $\text{K}_2\text{C}_6\text{O}_6$ is also up to 4 (Fig-

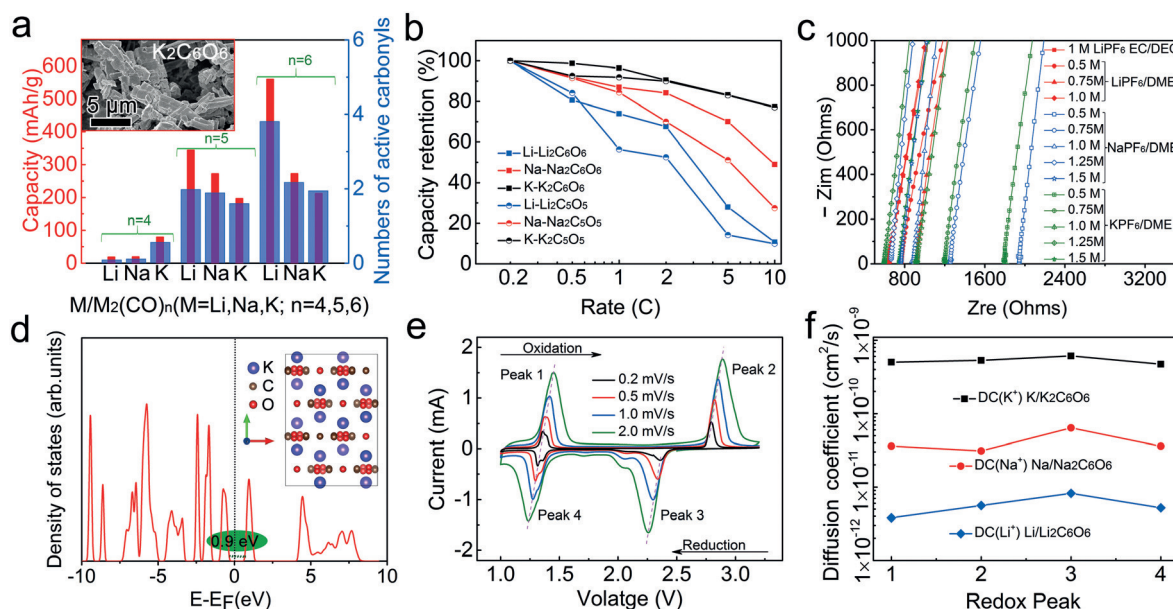


Figure 1. Electrochemical performance of oxocarbon salts in rechargeable batteries. a) Initial discharge capacity and corresponding use of carbonyl groups in the oxocarbon salts. The results were obtained with $\text{M}/\text{M}_2(\text{CO})_n$ batteries (M = Li, Na, K; $n = 4, 5, 6$). The current density is 0.2 C ($1 \text{ C} = 200 \text{ mA g}^{-1}$). The inset is a SEM image of $\text{K}_2\text{C}_6\text{O}_6$. b) Comparison of the capacity retention of $\text{M}/\text{M}_2(\text{CO})_n$ batteries at different current density. c) Characterization of the ionic conductivity of different concentrations of Li, Na, and K-ion electrolytes. d) Density of states (DOS) with crystal structures of $\text{K}_2\text{C}_6\text{O}_6$. e) Cyclic voltammetry (CV) curves of K/ $\text{K}_2\text{C}_6\text{O}_6$ battery at different scan rates. f) Comparison of diffusion coefficient of Li/ $\text{Li}_2\text{C}_6\text{O}_6$, Na/ $\text{Na}_2\text{C}_6\text{O}_6$ and K/ $\text{K}_2\text{C}_6\text{O}_6$ batteries. The electrodes were prepared with the active materials, super P and polyvinylidene fluoride (PVdF) with a mass ratio of 6:3:1. The mass loading of each electrode is about $1.5\text{--}2.0 \text{ mg cm}^{-2}$.

ure S12a,b), while the use in five-membered oxocarbon salts is nearly unchanged (Figure S13a–c). In general, the operation voltage of the oxocarbon salts increase from the four- to five- and six-membered ring salts (Figure S14), which is attributed to the gradually reduced energy of the lowest unoccupied molecular orbital (LUMO; Table S1) and is in accordance with the reported rules on dicarbonyl compounds.^[11] As a short summary of preliminary test on the nine oxocarbon salts, the four-membered ring oxocarbon salts reveal less activity for rechargeable batteries and $M_2(CO)_5$ is shown as the smallest ring for inserting metal ions.

Specially, the batteries with oxocarbon K-salts ($K_2C_5O_5$ and $K_2C_6O_6$) show fast K-ion reaction activities. The discharge capacities of K/ $K_2C_6O_6$ battery are 210, 205, 192, 177, 164 mA h g⁻¹ at current densities of 0.5 C, 1 C, 2 C, 5 C and 10 C, respectively (Figure S15c). The capacity retention of 10 C is close to 80 % of that at 0.2 C. Meanwhile, this superior high-rate performance is remained in the following cycling (Figure S16). However, the capacity retention of 10 C to 0.2 C for Na/ $Na_2C_6O_6$ battery is 49 % and it is only 11 % for Li/ $Li_2C_6O_6$ battery (Figure 1b). In addition, the K/ $K_2C_6O_6$ battery also reveals less voltage decrease at high current density than Na/ $Na_2C_6O_6$ and Li/ $Li_2C_6O_6$ (Figure S15a,b). This high rate performance is considered as the natural character of $K_2C_6O_6$. When we reduce the ratio of conductivity carbon (only 10 %), it also remains a capacity of 171 mA h g⁻¹ at 5 C (Figure S17). In addition, the high-rate performance of K/ $K_2C_5O_5$ battery is also much more outstanding than Li/ $Li_2C_5O_5$ and Na/ $Na_2C_5O_5$ batteries (Figure S18a–c). Furthermore, this rapid K-ion insertion activity is propagable for other organic electrodes (For instance, 1,4-anthraquinone, AQ). K-AQ battery also unfolds the best high-rate performance among metal-AQ batteries (Figure S19a–e).

To unravel the reasons of fast rate performance, the ionic conductivity of a different electrolyte concentration (Figure 1c and Table S2) was tested. Finally, we found that the 1.25 M KPF₆/DME (dimethoxyethane) electrolyte showed the highest ionic conductivity, exceeding the highest conductivity of Li-ion (1 M LiPF₆/EC (ethylene carbonate), DEC (diethyl carbonate)) and Na-ion (1.25 M NaPF₆/DME) electrolytes. Although the K ion has a larger ionic radius than Li and Na ions, the K ion is considered slightly soluble, which enables the fast motion of the K ion.^[9g] DFT calculations on the density of states (DOS) of $K_2C_6O_6$ were carried out. As illustrated in Figure 1d, the band gap of $K_2C_6O_6$ is 0.9 eV, which is narrower than that of $Na_2C_6O_6$ (Figure S20). This proves the inherent semiconductor feature of $K_2C_6O_6$. In addition, the order of electric conductivity is $K_2C_6O_6 > Na_2C_6O_6 > Li_2C_6O_6$, which agrees well with the rate performance (Figure S21). $K_2C_6O_6$ presents a typical layered structure.^[12] The K ion can diffuse between the layers and the electrons can easily transfer along the conjugated benzene ring layers. Furthermore, cyclic voltammetry (CV) measurement was applied to record the redox properties of the K/ $K_2C_6O_6$ battery from the second cycle. Two reduction peaks at 2.4 V/1.2 V and two oxidation peaks at 2.8 V/1.3 V can be observed (Figure 1e). The reduction peaks shift to lower potentials and the oxidation peaks shift to higher potentials

with the increase of scan rate, ascribing to the enhanced polarization by increasing scan rate. The diffusion coefficients of metal ion in $M_2C_6O_6$ were calculated with the Randles–Sevcik equation (details are given in the Supporting Information).^[13] We estimate two oxidation peaks and two reduction peaks of K/ $K_2C_6O_6$ batteries. The peak currents are linear with the square roots of scan rate (Figure S22). The diffusion coefficients of K ion calculated by the four peaks are about 5×10^{-10} cm² s⁻¹ (Figure 1f), which exceeds the diffusion coefficients of Li/ $Li_2C_6O_6$ (Figure S23a,b) and Na/ $Na_2C_6O_6$ (Figure S24a,b) batteries. The higher diffusion coefficients also imply the fast rate performance of the K/ $K_2C_6O_6$ battery. The intrinsic semiconductor character, high ionic conductivity K-ion electrolyte, and fast K-ion diffusion synergistically contribute to the fast rate performance of the K/ $K_2C_6O_6$ battery.

According to the discharge capacity, $K_2C_6O_6$ is able to undergo two-electron transfer reactions with $K_4C_6O_6$ as the discharge product (Figure 2a). This reaction mechanism is further confirmed by in situ Raman measurement (Figure 2b). For fresh electrodes (points 1), two major peak regions can be observed. The yellow region stands for the breathing vibration of the ring skeleton and the blue region stands for the vibration of the carbonyl compounds.^[14] The carbonyl compounds are the active groups because their vibration signals gradually fade with increasing discharge depth. Meanwhile, the vibration of ring breathing is well remained, which proves the molecular structural stability of $K_2C_6O_6$. During the charging process, the vibration of the carbonyl compound recurs to the original states, demonstrat-

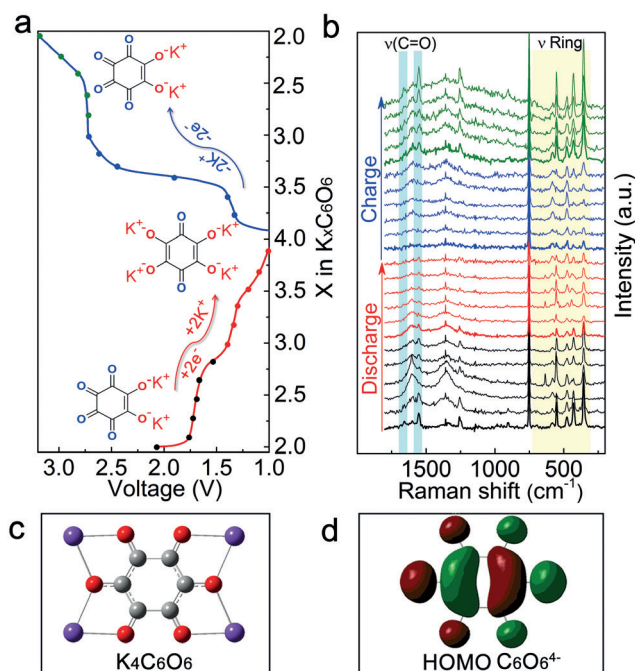


Figure 2. Characterization of the reaction mechanism of the K/ $K_2C_6O_6$ battery. a) Discharge/charge curves with marked points for in situ Raman tests. b) Corresponding Raman spectra. c) The most stable structure of the discharge product ($K_4C_6O_6$). d) HOMO plots of $C_6O_6^{4-}$.

ing the high reversibility of the $\text{K}/\text{K}_2\text{C}_6\text{O}_6$ battery. In addition, this reversible property was maintained in the following discharge/charge process (Figure S25). Two possible structures of $\text{K}_4\text{C}_6\text{O}_6$ exists after discharge. The inserted K ion can occupy the *para*- (Figure 2c) or *ortho*-positions (Figure S26) toward the original K-enolate groups ($-\text{OK}$). Finally, DFT calculation results reveal that the *para*-position is more favorable, which is 0.01057 a.u. lower than the *ortho* one. Plots of the highest occupied molecular orbital (HOMO) express the location of the valence-shell electron, which can be used to evaluate the stability of the organic compounds after gaining the electrons.^[15] The HOMO structure of $\text{C}_6\text{O}_6^{4-}$ does not alter, indicating the stability of $\text{K}_2\text{C}_6\text{O}_6$ after two-electrons reactions (Figure 2d). In summary, $\text{K}_2\text{C}_6\text{O}_6$ can insert two K-ions by forming $\text{K}_4\text{C}_6\text{O}_6$ in a discharge process. After charging, these two K ions can be reversibly extracted from the structures of $\text{K}_4\text{C}_6\text{O}_6$ to give $\text{K}_2\text{C}_6\text{O}_6$.

Inspired by the large interval between the initial and the second K-ion insertion, a first example of rocking-chair K-ion batteries with inorganic–organic electrode materials was realized. The $\text{K}/\text{K}_2\text{C}_6\text{O}_6$ battery can separately operate at different regions with suggested reaction of $\text{K}_3\text{C}_6\text{O}_6/\text{K}_4\text{C}_6\text{O}_6$ at a discharge platform of 1.3 V (anode reaction, Figure 3a) and $\text{K}_2\text{C}_6\text{O}_6/\text{K}_3\text{C}_6\text{O}_6$ at a discharge platform of 2.4 V (cathode reaction, Figure 3b). The $\text{K}_3\text{C}_6\text{O}_6$ is considered as a compound with radical, which has been confirmed by electron spin resonance (ESR) spectra (Figure S27). As a result, the constructed $\text{K}_4\text{C}_6\text{O}_6/\text{K}_2\text{C}_6\text{O}_6$ battery displays an operation voltage of 1.1 V (Figure 3c), corresponding to energy density of 35 Wh kg^{-1} (based on the mass of both cathode and anode). Although the capacity and working voltage still need

improvement, a state-of-the-art rocking-chair K-ion battery was obtained from inorganic–organic hybrid materials, which processes the advantages of high renewability and wide abundance. Moreover, $\text{K}_2\text{C}_6\text{O}_6$ can be directly prepared from the natural product myo-inositol and $\text{K}_4\text{C}_6\text{O}_6$ can be directly obtained through reaction of tetrahydroxy-quinone and KOCH_3 .^[5a,16] Thus, the K-ion battery with a rocking-chair reaction mechanism can be obtained without using K metal.

In summary, oxocarbon salts with different frameworks and metal ions have been used as electrodes in rechargeable (Li, Na, K) batteries. The working voltage and capacity are visually compared. As an intriguing result, we initially discovered the fast K-ion insertion/extraction properties at the $\text{K}_2\text{C}_6\text{O}_6$ cathode, which shows capacities of 212 mA h g^{-1} at 0.2 C and 164 mA h g^{-1} at 10 C. The narrow band-gap, high ionic conductivity of the K-ion electrolyte and the high diffusion K-ion coefficient synergistically contribute to these results. In addition, this high-rate performance can propagate towards other K-ion insertion materials. Moreover, a K-ion battery with rocking-chair reaction mechanism has been demonstrated. Considering the high abundance of K resource and the low standard electric potential of K^+/K , our finding not only provides an appealing chance for K-ion batteries but also opens a new way of developing sustainable materials for energy storage.

Acknowledgements

This work was supported by National NSFC (grant numbers 21231005 and 51231003), and MOE (grant numbers B12015 and IRT13R30).

Keywords: batteries · electrodes · molecular engineering · renewable materials · sustainable chemistry

How to cite: *Angew. Chem. Int. Ed.* **2016**, 55, 12528–12532
Angew. Chem. **2016**, 128, 12716–12720

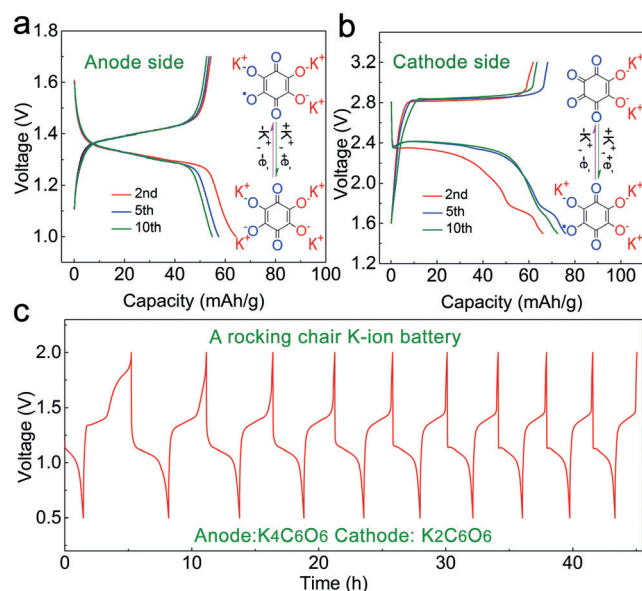


Figure 3. Properties of the rocking-chair K-ion battery. Discharge/charge curves of the $\text{K}/\text{K}_2\text{C}_6\text{O}_6$ battery at a) the anode region (1.0–1.7 V) and b) the cathode region (1.5–3.2 V). The inset shows the supposed reaction mechanism. c) The K-ion battery properties with $\text{K}_2\text{C}_6\text{O}_6$ as cathode and $\text{K}_4\text{C}_6\text{O}_6$ as anode. The current density is 25 mA g^{-1} and the cathode capacity is about 70 mA h g^{-1} . The mass loading of the anode is 1.2 times larger than that of the cathode.

- [1] a) M. Armand, J. M. Tarascon, *Nature* **2008**, 451, 652–657; b) N. S. Choi, Z. Chen, S. A. Freunberger, X. Ji, Y. K. Sun, K. Amine, G. Yushin, L. F. Nazar, J. Cho, P. G. Bruce, *Angew. Chem. Int. Ed.* **2012**, 51, 9994–10024; *Angew. Chem.* **2012**, 124, 10134–10166; c) Y. Ding, G. Yu, *Angew. Chem. Int. Ed.* **2016**, 55, 4772–4776; *Angew. Chem.* **2016**, 128, 4850–4854.
- [2] a) T. Janoschka, N. Martin, U. Martin, C. Friebe, S. Morgenstern, H. Hiller, M. D. Hager, U. S. Schubert, *Nature* **2015**, 527, 78–81; b) K. Lin, Q. Chen, M. R. Gerhardt, L. Tong, S. B. Kim, L. Eisenach, A. W. Valle, D. Hardee, R. G. Gordon, M. J. Aziz, M. P. Marshak, *Science* **2015**, 349, 1529–1532; c) J. Liu, P. Kopold, P. A. van Aken, J. Maier, Y. Yu, *Angew. Chem. Int. Ed.* **2015**, 54, 9632–9636; *Angew. Chem.* **2015**, 127, 9768–9772; d) W. Huang, Z. Zhu, L. Wang, S. Wang, H. Li, Z. Tao, J. Shi, L. Guan, J. Chen, *Angew. Chem. Int. Ed.* **2013**, 52, 9162–9166; *Angew. Chem.* **2013**, 125, 9332–9336; e) B. Häupler, A. Wild, U. S. Schubert, *Adv. Energy Mater.* **2015**, 5, 1402034; f) Y. Morita, S. Nishida, T. Murata, M. Moriguchi, A. Ueda, M. Satoh, K. Arifuku, K. Sato, T. Takui, *Nat. Mater.* **2011**, 10, 947–951; g) Z. Song, H. Zhan, Y. Zhou, *Angew. Chem. Int. Ed.* **2010**, 49, 8444–8448; *Angew. Chem.* **2010**, 122, 8622–8626; h) J. Hong, M. Lee, B. Lee, D. H. Seo, C. B. Park, K. Kang, *Nat. Commun.* **2014**, 5, 5335; i) H. Wu, Q. Meng, Q. Yang, M. Zhang, K. Lu, Z. Wei,

- Adv. Mater.* **2015**, *27*, 6504–6510; j) Y. Zhao, Y. Ding, J. Song, G. Li, G. Dong, J. B. Goodenough, G. Yu, *Angew. Chem. Int. Ed.* **2014**, *53*, 11036–11040; *Angew. Chem.* **2014**, *126*, 11216–11220; k) J. Wu, X. Rui, G. Long, W. Chen, Q. Yan, Q. Zhang, *Angew. Chem. Int. Ed.* **2015**, *54*, 7354–7358; *Angew. Chem.* **2015**, *127*, 7462–7466; l) H. Wang, P. Hu, J. Yang, G. Gong, L. Guo, X. Chen, *Adv. Mater.* **2015**, *27*, 2348–2354; m) A. Shimizu, Y. Tsujii, H. Kuramoto, T. Nokami, Y. Inatomi, N. Hojo, J. Yoshida, *Energy Technol.* **2014**, *2*, 155–158; n) Z. Zhu, M. Hong, D. Guo, J. Shi, Z. Tao, J. Chen, *J. Am. Chem. Soc.* **2014**, *136*, 16461–16464; o) K. Oyaizu, H. Nishide, *Adv. Mater.* **2009**, *21*, 2339–2344; p) Y. Ding, Y. Zhao, G. Yu, *Nano Lett.* **2015**, *15*, 4108–4113; q) J. Lee, H. Kim, M. J. Park, *Chem. Mater.* **2016**, *28*, 2408–2416.
- [3] a) Y. Liang, Z. Tao, J. Chen, *Adv. Energy Mater.* **2012**, *2*, 742–769; b) Z. Song, H. Zhou, *Energy Environ. Sci.* **2013**, *6*, 2280–2301; c) K. Zhang, C. Guo, Q. Zhao, Z. Niu, J. Chen, *Adv. Sci.* **2015**, *2*, 1500018; d) T. B. Schon, B. T. McAllister, P. F. Li, D. S. Seferos, *Chem. Soc. Rev.* **2016**, DOI: 10.1039/C6CS00173D.
- [4] a) H. Chen, M. Armand, M. Courty, M. Jiang, C. P. Grey, F. Dolhem, J. M. Tarascon, P. Poizot, *J. Am. Chem. Soc.* **2009**, *131*, 8984–8988; b) B. Genorio, K. Pirnat, R. Cerc-Korosec, R. Dominko, M. Gaberscek, *Angew. Chem. Int. Ed.* **2010**, *49*, 7222–7224; *Angew. Chem.* **2010**, *122*, 7380–7382; c) X. Han, C. Chang, L. Yuan, T. Sun, J. Sun, *Adv. Mater.* **2007**, *19*, 1616–1621; d) K. Zhang, Z. Hu, Z. Tao, J. Chen, *Sci. China Mater.* **2014**, *57*, 42–58; e) C. Wang, Y. Xu, Y. Fang, M. Zhou, L. Liang, S. Singh, H. Zhao, A. Schober, Y. Lei, *J. Am. Chem. Soc.* **2015**, *137*, 3124–3130; f) M. Armand, S. Grugeon, H. Vezin, S. Laruelle, P. Ribiere, P. Poizot, J. M. Tarascon, *Nat. Mater.* **2009**, *8*, 120–125; g) Z. Tu, P. Nath, Y. Lu, M. D. Tikekar, L. A. Archer, *Acc. Chem. Res.* **2015**, *48*, 2947–2956; h) Q. Zhao, C. Guo, Y. Lu, L. Liu, J. Liang, J. Chen, *Ind. Eng. Chem. Res.* **2016**, *55*, 5795–5804.
- [5] a) H. Chen, M. Armand, G. Demailly, F. Dolhem, P. Poizot, J. M. Tarascon, *ChemSusChem* **2008**, *1*, 348–355; b) H. Kim, D. H. Seo, G. Yoon, W. A. Goddard, Y. S. Lee, W. S. Yoon, K. Kang, *J. Phys. Chem. Lett.* **2014**, *5*, 3086–3092; c) X. Wu, S. Jin, Z. Zhang, L. Jiang, L. Mu, Y. S. Hu, H. Li, X. Chen, M. Armand, L. Chen, X. Huang, *Sci. Adv.* **2015**, *1*, e1500330–e1500330; d) Y. Wang, Y. Ding, L. Pan, Y. Shi, Z. Yue, G. Yu, *Nano Lett.* **2016**, *16*, 3329–3334; e) K. Chihara, N. Chujo, A. Kitajou, S. Okada, *Electrochim. Acta* **2013**, *110*, 240–246; f) C. Wang, Y. Fang, Y. Xu, L. Liang, M. Zhou, H. Zhao, Y. Lei, *Adv. Funct. Mater.* **2016**, *26*, 1777–1786; g) C. Luo, R. Huang, R. Kevorkyants, M. Pavanello, H. He, C. Wang, *Nano Lett.* **2014**, *14*, 1596–1602.
- [6] a) N. Ogihara, T. Yasuda, Y. Kishida, T. Ohsuna, K. Miyamoto, N. Ohba, *Angew. Chem. Int. Ed.* **2014**, *53*, 11467–11472; *Angew. Chem.* **2014**, *126*, 11651–11656; b) T. Yasuda, N. Ogihara, *Chem. Commun.* **2014**, *50*, 11565–11567; c) S. Wang, L. Wang, Z. Zhu, Z. Hu, Q. Zhao, J. Chen, *Angew. Chem. Int. Ed.* **2014**, *53*, 5892–5896; *Angew. Chem.* **2014**, *126*, 6002–6006; d) S. E. Burkhardt, J. Bois, J.-M. Tarascon, R. G. Hennig, H. D. Abruña, *Chem. Mater.* **2013**, *25*, 132–141; e) S. Wang, L. Wang, K. Zhang, Z. Zhu, Z. Tao, J. Chen, *Nano Lett.* **2013**, *13*, 4404–4409; f) A. Shimizu, H. Kuramoto, Y. Tsujii, T. Nokami, Y. Inatomi, N. Hojo, H. Suzuki, J. Yoshida, *J. Power Sources* **2014**, *260*, 211–217.
- [7] a) W. Wan, H. Lee, X. Yu, C. Wang, K. W. Nam, X. Q. Yang, H. Zhou, *RSC Adv.* **2014**, *4*, 19878–19882; b) M. Yao, K. Kuratani, T. Kojima, N. Takeichi, H. Senoh, T. Kiyobayashi, *Sci. Rep.* **2014**, *4*, 3650; c) L. Zhu, Y. Shen, M. Sun, J. Qian, Y. Cao, X. Ai, H. Yang, *Chem. Commun.* **2013**, *49*, 11370–11372.
- [8] a) R. West, D. L. Powell, *J. Am. Chem. Soc.* **1963**, *85*, 2577–2579; b) X. Bao, X. Zhou, C. Flener Lovitt, A. Venkatraman, D. A. Hrovat, R. Gleiter, R. Hoffmann, W. T. Borden, *J. Am. Chem. Soc.* **2012**, *134*, 10259–10270.
- [9] a) X. Ren, Y. Wu, *J. Am. Chem. Soc.* **2013**, *135*, 2923–2926; b) D. Trauner, *Angew. Chem. Int. Ed.* **2003**, *42*, 5671–5675; *Angew. Chem.* **2003**, *115*, 5849–5853; c) Q. Zhao, Y. Hu, K. Zhang, J. Chen, *Inorg. Chem.* **2014**, *53*, 9000–9005; d) Z. Jian, Z. Xing, C. Bommier, Z. Li, X. Ji, *Adv. Energy Mater.* **2016**, *6*, 1501874; e) X. Lu, M. E. Bowden, V. L. Sprenkle, J. Liu, *Adv. Mater.* **2015**, *27*, 5915–5922; f) C. D. Wessells, S. V. Peddada, R. A. Huggins, Y. Cui, *Nano Lett.* **2011**, *11*, 5421–5425; g) S. Komaba, T. Hasegawa, M. Dahbi, K. Kubota, *Electrochem. Commun.* **2015**, *60*, 172–175; h) W. Luo, J. Wan, B. Ozdemir, W. Bao, Y. Chen, J. Dai, H. Lin, Y. Xu, F. Gu, V. Barone, L. Hu, *Nano Lett.* **2015**, *15*, 7671–7677; i) Z. Jian, W. Luo, X. Ji, *J. Am. Chem. Soc.* **2015**, *137*, 11566–11569.
- [10] a) Y. Chen, W. Luo, M. Carter, L. Zhou, J. Dai, K. Fu, S. Lacey, T. Li, J. Wan, X. Han, Y. Bao, L. Hu, *Nano Energy* **2015**, *18*, 205–211; b) Z. Xing, Z. Jian, W. Luo, Y. Qi, C. Bommier, E. S. Chong, Z. Li, L. Hu, X. Ji, *Energy Storage Mater.* **2016**, *2*, 63–68.
- [11] T. Nokami, T. Matsuo, Y. Inatomi, N. Hojo, T. Tsukagoshi, H. Yoshizawa, A. Shimizu, H. Kuramoto, K. Komae, H. Tsuyama, J. Yoshida, *J. Am. Chem. Soc.* **2012**, *134*, 19694–19700.
- [12] J. A. Cowan, J. A. K. Howard, *Acta Cryst.* **2004**, *E60*, m511–m513.
- [13] a) J. E. B. Randles, *Trans. Faraday Soc.* **1948**, *44*, 327–338; b) A. Sevcik, *Collect. Czech. Chem. Commun.* **1948**, *13*, 349.
- [14] N. L. G. D. Souza, T. F. Salles, H. M. Brandão, H. G. M. Edwards, L. F. C. d. Oliveira, *J. Braz. Chem. Soc.* **2015**, *26*, 1247–1256.
- [15] a) G. Wang, S. Yuan, Z. J. Si, X. B. Zhang, *Energy Environ. Sci.* **2015**, *8*, 3160–3165; b) Y. Liang, P. Zhang, J. Chen, *Chem. Sci.* **2013**, *4*, 1330–1337; c) T. Ma, Q. Zhao, J. Wang, Z. Pan, J. Chen, *Angew. Chem. Int. Ed.* **2016**, *55*, 6428–6432; *Angew. Chem.* **2016**, *128*, 6538–6542.
- [16] R. West, H. Y. Niu, *J. Am. Chem. Soc.* **1962**, *84*, 1324–1325.

Received: July 25, 2016

Revised: August 25, 2016

Published online: September 8, 2016